Anode Power Deposition in an AF-MPDT with Two Unique Magnetic Field

IEPC-2019-A401

Presented at the 36th International Electric Propulsion Conference
University of Vienna • Vienna, Austria
September 15-20, 2019

Peng Wu[1], Yibai Wang [2], Zhiyuan Chen [3]
School of Astronautics, Biehang University, Beijing, 100083, China

Baojun Wang[4]
Beijing Institute of Control Engineering and, Beijing, 100080, China

Haibin Tang[5]
School of Space and Environment, Beihang University, Beijing, 100083, China

Abstract: The applied field magnetoplasmadynamic thruster (AF-MPDT) is one of the most promising high-power electric thrusters that could be used in the future deep space missions. The anode power deposition is an urgent problem in the operation of AF-MPDTs, which would cause significant power loss near the anode surface. In order to improve the performance of AF-MPDTs, two unique magnetic fields: discharge chamber enhanced magnetic field (DCEMF) and magnetic nozzle enhanced magnetic field (MNEMF) are proposed in this paper. The discharge voltage, the anode and cathode power deposition at variation of coil magnetic strength are presented in this paper. The influence of the discharge current and mass flowrate is also investigated. According to the experimental results, the anode power deposition decreases with the increase mass flow rate in quadratic polynomial mode. Furthermore, the thruster performance in DCEMF has the best performance for the highest discharge voltage and low anode power deposition ratio.

V_d	=	discharge voltage
I	=	discharge current
B	=	magnetic strength
B_c	=	magnetic strength generated by coil
m	=	mass flow rate

I.Introduction

Applied field Magnetoplasmadynamic Thruster (AF-MPDT) is a kind of device which converts electrical energy into propellant axial kinetic energy by an external magnetic field. It is considered as one of the potential electric propulsion devices for deep space exploration because of its wide range of thrust levels (0.1-10N) and high thrust efficiency (up to 67%) in hundred-kilowatt [1-4]. However, there is a significant energy loss that limits the wide application of the AF-MPDT, which is called anode power deposition. Anode power deposition is an essential power loss in AF-MPDT operating at hundred-kilowatt power levels. For powers below one megawatt, the loses in the anode can range from 40% to 90% of the total thruster power[5]. The anode power deposition is mainly composed by the

[1] PhD Student, School of Astronautics, 13151149@buaa.edu.cn.
[2] Associate Professor, School of Astronautics, wangyibai@buaa.edu.cn.
[3] PhD Student, School of Astronautics, chenzhiyuan@buaa.edu.cn.
[4] Engineer, Beijing Institute of Control Engineer, wangbaojun@buaa.edu.cn.
[5] Professor, School of Space and Environment, thb@buaa.edu.cn.

anode heating from the anode fall, the random electron thermal energy, the heat released due to the work function of the anode material, the cathode radiation, and the plasma heat transfer[6]. The contribution to anode heating from the anode voltage drop is the most important mechanism of the anode power deposition[7].

A lot of theoretical research about the anode power deposition of AF-MPDT have been published in recent decades. A finite element discretized two-dimensional self-consistent formulation of plasma–sheath dynamics, using multi-fluid equations for partially ionized plasma was proposed by Roy to compute the potential distribution along the electrode[8]. Ahangar developed an analytical approach to analyze the anode thermal process in a self-field MPD thruster, including effects of both non-neutral and quasi-neutral plasma regions near the anode surface[7]. The relations between the voltage drop and current density along the anode lip were computed in this article. The results of these researches have a good agreement with the experiments. According to their research, the anode fall will rise with an increase in the magnetic strength. Zefeng Li suggested that the decrease of the anode fall voltage can improve the performance of the AF-MPDT[9]. It is concluded that varying the magnetic field near the anode surface may reduce the anode power deposition.

Many experiments have also been done to investigate the anode power deposition. A.D. Gallimore did deep research about the anode power deposition by experimentation[10-13]. For AF-MPDT and pulsed quasi-steady MPDT, there are 42% and 70% power deposited in the anode due to the anode heating respectively. Myers investigated the effects of current and applied magnetic field on anode voltage drop separately by experimental methods. The anode fall was shown to increase with the current and magnetic field[5]. Gallimore also found a way to reduce the anode power deposition in SF-MPDT. According to Gallimore[14], reducing the azimuthal magnetic strength near the anode surface can decreasing the anode power deposition in SF-MPDT. In order to improve the performance of AF-MPDT, a permanent magnet was placed in the anode water-cooling chamber in this paper. As shown in Figure 1, the magnetic field of permanent magnet is quite different with coil. The N40 RbFeB permanent magnet has an inner and outer diameter of 62 and 78 mm, and is 25 mm long. There are two opposite direction of magnetic lines in permanent magnet, which means that two different distribution may be formed when the direction of coil is changed: discharge chamber enhanced magnetic field (DCEMF) and magnetic nozzle enhanced magnetic field (MNEMF). The performance of AF-MPDT under which magnetic field will be better is worth to investigated.

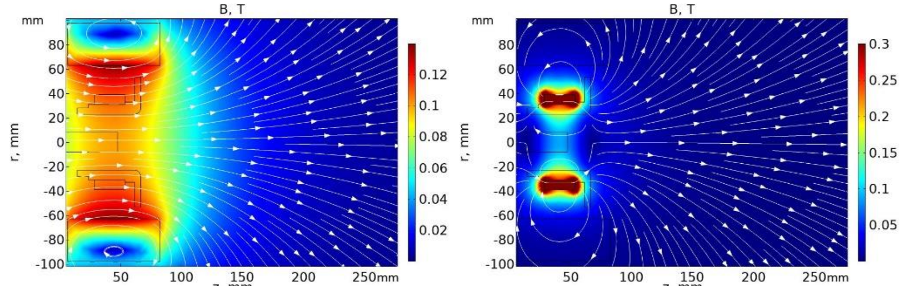

Figure 1 Magnetic field of coil(left) and Permanent magnet (right)

This research aims to estimate the performance of MAT-50 at three kind of magnetic field: traditional magnetic field (TMF), discharge chamber enhanced magnetic field and magnetic nozzle enhanced magnetic field. The discharge voltage, the anode and cathode power deposition at variation of coil magnetic strength are presented in this paper. The influence of the discharge current and mass flow rate is also investigated.

II.Experimental Facility

A. Testing Facility

As shown in Figure 2, the experimental investigations on AF-MPDT were done in electric propulsion testing facility system 3 (JLPP). This system includes three subsystems: the vacuum system, the power source system and the water-cooling system. The vacuum system is composed by a vacuum tank that is 5m long with an inner diameter of 2.5m, two oil diffusion pumps and four mechanical pumps. The pump speed is 64000 L/s. The environment pressure can be maintained under 0.05 Pa when the flow rate of (argon) propellant is no more than 21 mg/s. The power source system provides a high voltage pulse to ignite the thruster, provides power for the thruster to accelerate the plasma, and provides power for the magnetic field coil to sustain the external magnetic field. The power source system consists of an ignition power source, a thruster power source, a coil power source and cables. The ignition power source can provide 8 kV or 15 kV discharge voltage. The thruster power source provides a direct current up to 200 A. The coil power source provides a direct current up to 150 A. The water-cooling system can provide cool high-pressure water to exchange the heat of the thruster, magnetic coil and power sources. This system consists of pumps group, water tank, compressor, water supply pipelines and pumps controllers.

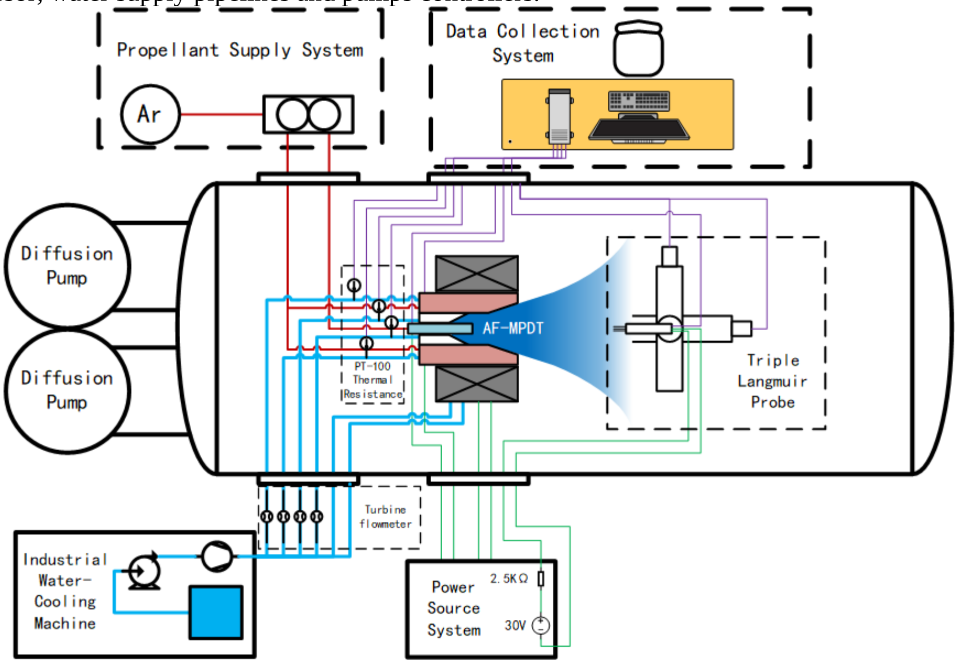

Figure 2 Schematic diagram of experiment system

B. Thruster MAT-50

The structure of the MAT-50 is shown in Figure 3. This thruster features a flat anode which has a water-cooling structure to exchange the heat from the anode surface and protect the permanent magnet. The copper anode assembly consists of three parts connected by bolts, and the graphite is used for sealing. The anode has an inner and outer diameter of 46 and 107 mm, respectively, and is 50 mm long. Propellant is injected through two anode pipes and one cathode pipe. The cathode, constructed out of tungsten, is 30 mm long (inside the discharge chamber) and 16 mm in diameter, and is held in place by a water-cooled copper structure. There are seven channels in cathode, and each channel is 1.7 mm in diameter. The insulator between anode and cathode is made of boron nitride. Other insulation parts are realized with PEEK.

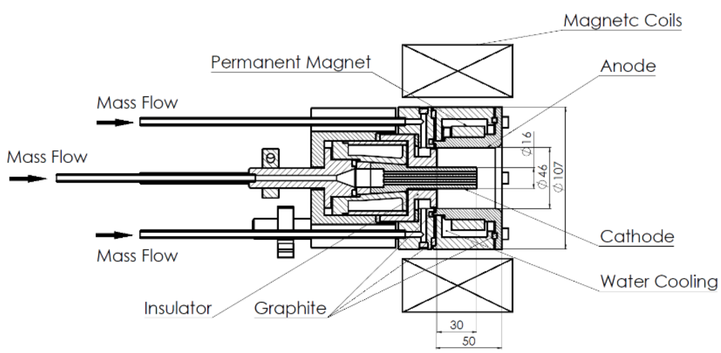

Figure 3 Schematic view of model MAT-50

C. Measurement of electrode power deposition

The electrode power deposition is calculated by the differences of the inlet and outlet water temperature. As shown in Figure 2, there are four PT-100 thermal resistances placed in the anode and cathode water cooling channel respectively. The temperature transmitter of the PT-100 provides measurements accurate to within 0.25%. Cooling water flow rates for each water-cooling channel are monitored with turbine flowmeters, which provide measurements accurate to within 1.5%. The power deposition can be given by Eq.(1).

$$P = c\dot{m}\Delta T \tag{1}$$

where P is the power deposition, c is the specific heat capacity, and ΔT is the temperature difference between inlet cooling-water and outlet cooling-water.

D. Magnetic field of MAT-50

The magnetic strength distribution of discharge chamber enhanced magnetic field and magnetic nozzle enhanced magnetic field is shown in Figure 4 and Figure 5 respectively.

Compared with Figure 1, the discharge chamber enhanced magnetic field and magnetic nozzle enhanced magnetic field is quite different with traditional one. A convergent-divergent-convergent (C-D-C) magnetic field is formed in MNEMF, and D-C one is formed in the discharge chamber enhanced magnetic field. In the MNEMF, the magnetic strength is increased 0.015T at the exit of the thruster and decreased 0.08T at cathode tip, which is opposite in DCEMF, as shown in Figure 6 and Figure 7.

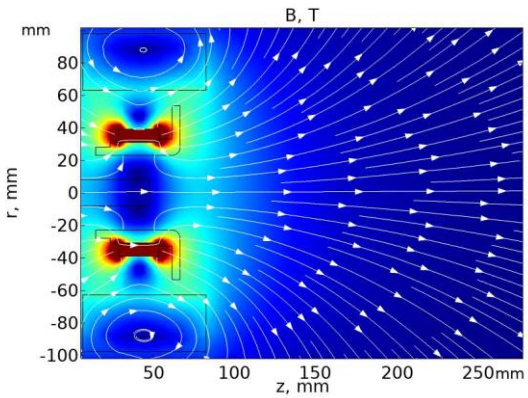

Figure 4 Magnetic strength distribution of magnetic nozzle enhanced magnetic field

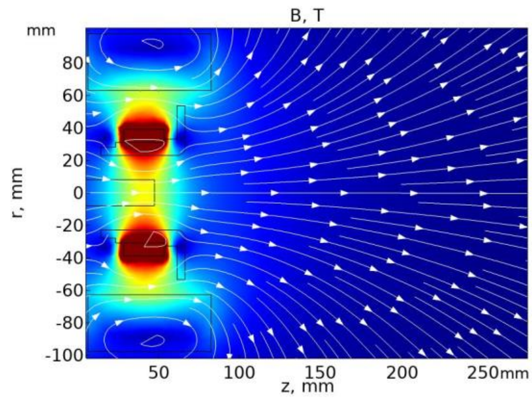

Figure 5 Magnetic strength distribution of discharge chamber enhanced magnetic field

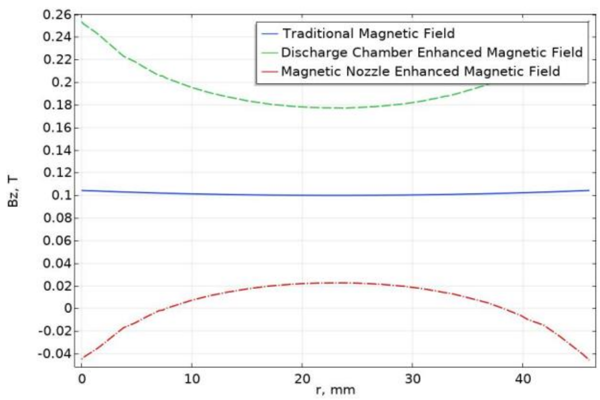

Figure 6 Distribution of axial magnetic strength in radial direction at cathode tip

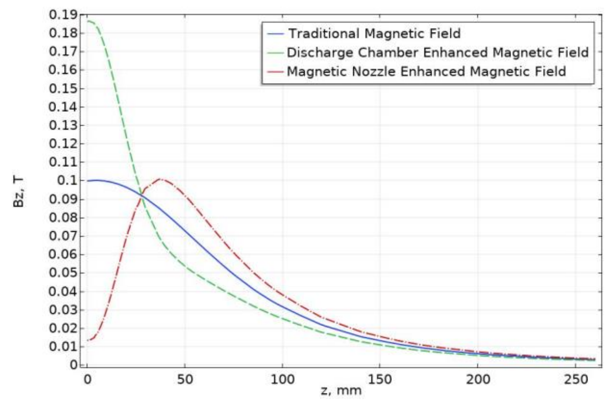

Figure 7 Distribution of axial magnetic strength in axial direction

III.Experimental Results

A. Operating conditions of electrode power deposition tests

Thruster operating conditions are listed in Table 1.

Table 1 Thruster operating conditions during the experiment.

Part 1 (I=150A, $\dot{m} = 21$mg/s)	Magnetic Field	Magnetic Strength Generated by Coil (mT)			
	TMF	50	75	100	125
	DCEMF				
	MNEMF				
Part 2 (B=125 mT)	Discharge Current	Total Mass Flow Rate (mg/s)			
	150A	21	25.2	33.6	42
	175A				
	200A				

B. Variation of Magnetic Strength Generated by Coil

As shown in Figure 8, when the time is 180s, the heat taken away by the cooling water from the electrode no longer changes. It is indicated that the anode and cathode of the thruster reach the heat balance with the cooling water at this time. The power deposited in the anode is seven times larger than it in the cathode. The anode power deposition is the most significant power loss in AF-MPDT.

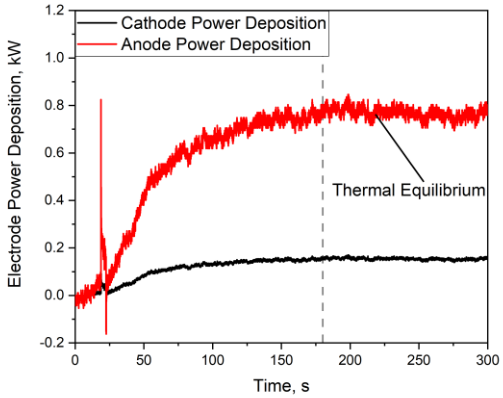

Figure 8 Electrode power deposition as a function of time in DCEMF, B=0.125mT

Table 2 and

Figure 9 show that, the permanent magnetic reduced the power deposition of both cathode and anode apparently. The anode power deposition in TMF is 1 kW larger than it in DCEMF and three times as it in MNEMF, when B_c is larger than 100 mT. The cathode power deposition in DCEMF is the lowest and maintained at 0.25 kW. The cathode power deposition in MNEMF decreases slightly with the rise of B_c and is larger than it in DCEMF. Although the anode power deposition is the lowest in MNEMF, the performance of the thruster in MNEMF is not the best because of the low discharge voltage, according to Figure 10 and Figure 11. The ratio of the anode power deposition to total power decreases with the rise of B_c in MNEMF. It is indicated that when B is larger than 125 mT, the MAT-50 may have the highest efficiency in MNEMF.

Table 2 Cathode power deposition at different Bc

Bc	TMF	MNEMF	DCEMF
50mT	0.1219	0.4661	0.2496
75mT	0.4105	0.1985	0.2948
100mT	0.5863	0.3954	0.2181

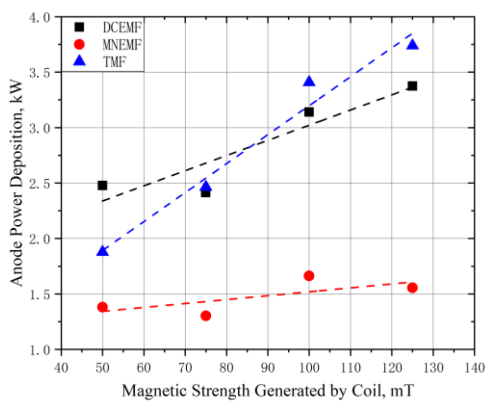

Figure 9 Anode Power Deposition vs Magnetic Strength Generated by Coil

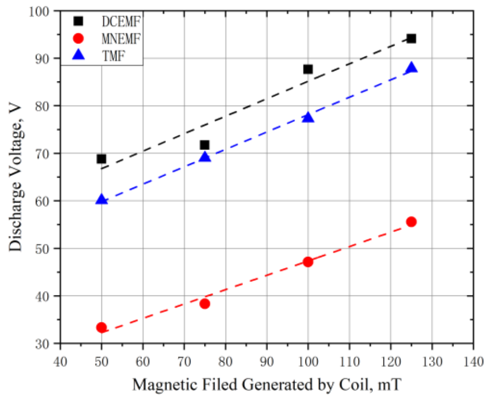

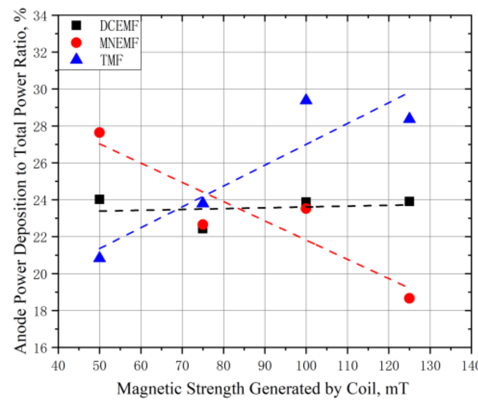

Figure 10 Discharge Voltage vs Magnetic Strength Generated by Coil

Figure 11 Anode Power Deposition to Total Power Ratio vs Magnetic Strength Generated by Coil

Although axial magnetic strength in DCEMF is much higher than it in TMF, the anode power deposition is lower, according to Figure 12 and

Figure 9. This may caused by the the low cathode temperature in DCEMF. The cathode power depositon in DCEMF is just almost half of it in TMF. It is claimed that the anode power deposition generated by cathode radiation and the anode heating from the anode fall are almost the same in Gallimore's research (B_c=80mT, I=850A) [13]. The cathode radiation may play a more important role in MAT-50. The imcrease of anode power deposition related to the axial magnetic strength may be smaller than the decrease of it caused by cathode radiation. According to

Figure 9 and Figure 13 The anode power deposition in MNEMF is the lowest which is because the low cathode radiation and the lowest axial magnetic strength.

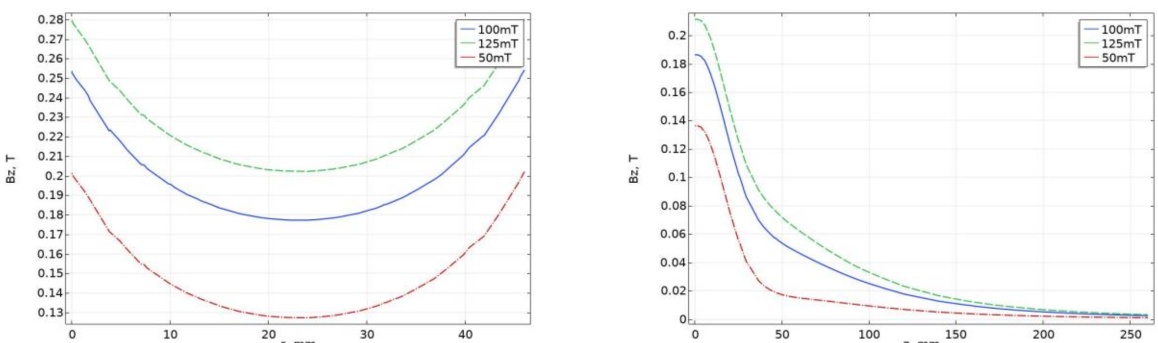

Figure 12 DCEMF Axial magnetic strength distribution in radial direction (left) and axial direction (right)

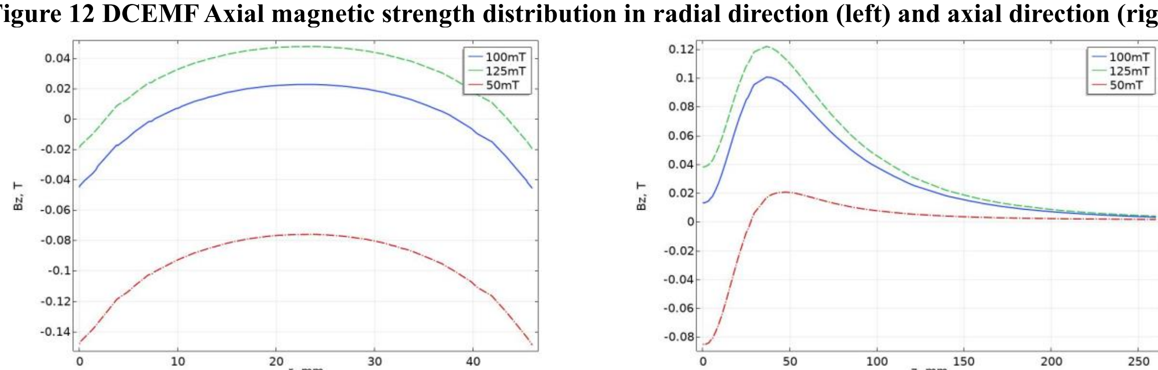

Figure 13 MNEMF Axial magnetic strength distribution in radial direction (left) and axial direction (right)

C. Variation of discharge current and mass flow rate

Table 3 Cathode power deposition at different I and m

I	21mg/s	33.6mg/s	42mg/s
150A	0.1219	0.4661	0.2496
175A	0.4105	0.1985	0.2948

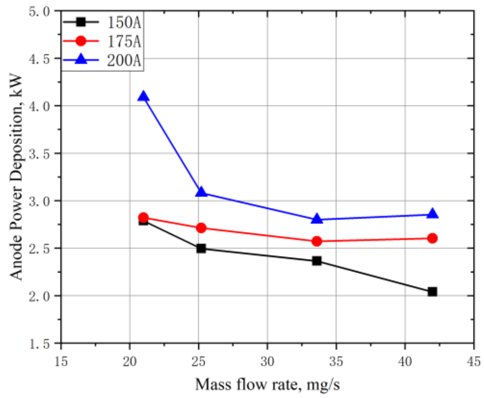

Figure 14 Anode Power Deposition vs Mass Flow Rate

As shown in Table 3 and

Figure **14**, the power deposition of cathode and anode increase with the rise of the discharge current. The larger discharge current needs higher cathode temperature, which account for the increase of the electrode deposition. The large current also increase the Lorentz force, which may compress the plasma near the anode to the middle. The decrease of the electron density near the anode may also increase the anode power deposition. The anode power deposition decreases with the increase mass flow rate in quadratic polynomial mode. There may be a suitable mass flow rate at which the thruster has the highest efficiency at a certain magnetic strength.

IV.Conclusion

In this paper, the performance of MAT-50 at three kind of magnetic field: traditional magnetic field (TMF), discharge chamber enhanced magnetic (DCEMF) field and magnetic nozzle enhanced magnetic field (MNEMF) is investigated. The discharge voltage, the anode and cathode power deposition at variation of coil magnetic strength are presented in this paper. The influences of the discharge current and mass flowrate are also presented. The anode power deposition in MNEMF is the lowest, however the performance of the thruster in it is not the best because of the high cathode temperature and low discharge voltage. The MAT-50 performance in DCEMF has the best performance for the highest discharge voltage and low anode power deposition ratio. The power deposition of anode increase with the rise of the discharge current. As the increase of the mass flow rate, the anode power deposition will decrease in quadratic polynomial mode.

Although the DCEMF is an effective magnetic field to improve the performance of AF-MPDT, the mechanism in it is still unclearly. The further analysis should be done in next work.

Acknowledgments

This work was supported by the National Natural Science Foundation of China (Grant No. 11872093).

References

[1] Tikhonov V B, Semenikhin S A, Brophy J R and Polk J E 1997 Performance of 130 kw MPD thruster with an external magnetic field and Li as propellant. In: *Proceedings of the 25 th International Electric Propulsion Conference*, pp 728-33

[2] Kodys A and Choueiri E 2005 A Critical Review of the State-of-the-Art in the Performance of Applied-Field Magnetoplasmadynamic Thrusters. In: *41st AIAA/ASME/SAE/ASEE Joint Propulsion Conference & Exhibit*, p 4247

[3] LaPointe M, Strzempkowski E and Pencil E 2004 High Power MPD Thruster Performance Measurements. In: *40th AIAA/ASME/SAE/ASEE Joint Propulsion Conference and Exhibit*,

[4] Wang B, Tang H, Wang Y, Lu C, Zhou C, Dong Y, Wang G, Cong Y, Luu D and Cao J 2018 A 100 KW Class Applied-field Magnetoplasmadynamic Thruster *J Vis Exp*

[5] Myers R and Soulas G 1992 Anode power deposition in applied-field MPD thrusters. In: *28th Joint Propulsion Conference and Exhibit,*

[6] Saber A J 1974 Anode power in a quasi-steady MPD thruster. Princeton

[7] Ahangar M 2017 Analytical investigation of anode heat flux in a magnetoplasmadynamic thruster *Applied Thermal Engineering* **118** 73-81

[8] Roy S 2004 Self-consistent Electrode Model for Magnetoplasmadynamic Thrusters. In: *40th AIAA/ASME/SAE/ASEE Joint Propulsion Conference and Exhibit,*

[9] Li Z, Tang H, Wang Y, Wang1 B, Lu X and Zhang Z 2018 Increasing the effective voltage in applied-field MPD thrusters *Journal of Physics D: Applied Physics*

[10] Gallimore A D 1991 Anode Power Deposition in MPD Thrusters

[11] Gallimore A D, Kelly A J and Jahn R G 1992 Anode power deposition in quasisteady magnetoplasmadynamic thrusters *Journal of Propulsion and Power* **8** 1224-31

[12] Gallimore A D, Kelly A J and Jahn R G 1993 Anode power deposition in magnetoplasmadynamic thrusters *Journal of Propulsion and Power* **9** 361-8

[13] Gallimore A D, Myers R M, Kelly A J and Jahn R G 1994 Anode power deposition in an applied-field segmented anode MPD thruster *Journal of Propulsion and Power* **10** 262-8

[14] Gallimore A, Kelly A and Jahn R 1992 Anode power deposition in a MPD thruster with a magnetically annulled Hall parameter anode. In: *28th Joint Propulsion Conference and Exhibit,*